TITLE PAGE

TITLE: Spatiotemporal dynamics of postoperative functional plasticity in patients with brain tumors in language areas

AUTHORS: Mikel Lizarazu[1,2], Santiago Gil-Robles[3,4], Iñigo Pomposo[4], Sanjeev Nara[1], Lucía Amoruso[1], Ileana Quiñones[1] and Manuel Carreiras[1,5,6]

AUTHOR AFFILIATIONS:

[1]BCBL, Basque Center on Cognition, Brain and Language, Donostia/San Sebastián, Spain

[2]Laboratoire de Sciences Cognitives et Psycholinguistique (ENS, EHESS, CNRS), Ecole Normale Supérieure, PSL Research University, Paris, France

[3]Department of Neurosurgery, Hospital Quirón, Madrid, Spain

[4]BioCruces Research Institute, Bilbao Spain

[5]Ikerbasque, Basque Foundation for Science, Bilbao, Spain

[6]University of the Basque Country, UPV/EHU, Bilbao, Spain

ADDRESS OF THE CORRESPONDING AUTHOR

Mikel Lizarazu

Basque Center on Cognition, Brain and Language

Mikeletegi Pasealekua, 69, 20009 Donostia/San Sebastián, Spain

e-mail: m.lizarazu@bcbl.eu

ABSTRACT

Postoperative functional neuroimaging provides a unique opportunity to investigate the neural mechanisms that facilitate language network reorganization. Previous studies in patients with low grade gliomas (LGGs) in language areas suggest that postoperative recovery is likely due to functional neuroplasticity in peritumoral and contra-tumoral healthy regions, but have attributed varying degrees of importance to specific regions. In this study, we used Magnetoencephalography (MEG) to investigate functional connectivity changes in peritumoral and contra-tumoral regions after brain tumor resection. MEG recordings of cortical activity during resting-state were obtained from 12 patients with LGGs in left-hemisphere language brain areas. MEG data were recorded before (Pre session), and 3 (Post_1 session) and 6 (Post_2 session) months after awake craniotomy. For each MEG session, we measured the functional connectivity of the peritumoral and contra-tumoral regions to the rest of the brain across the 1 to 100 Hz frequency band. We found that functional connectivity in the Post_1 and Post_2 sessions was higher than in the Pre session only in peritumoral regions and within the alpha frequency band. Functional connectivity in peritumoral regions did not differ between the Post_1 and Post_2 sessions. Alpha connectivity enhancement in peritumoral regions was observed in all patients regardless of the LGG location. Together, these results suggest that postoperative language functional reorganization occurs in peritumoral regions regardless of the location of the tumor and mostly develops within 3 months after surgery.

Keywords: Language networks; Low-grade glioma; Functional reorganization, Functional Connectivity, Magnetoencephalography.

SIGNIFICANCE STATEMENT

The human brain has an amazing ability to reorganize language networks by moving functions from a damaged area of the brain to other undamaged areas. Previous neuroimaging studies in patients with LGGs in language areas have suggested that recovery from postoperative difficulties is driven by functional neuroplasticity in peritumoral and contra-tumoral healthy regions. In the present study, we measured functional connectivity between peritumoral and contra-tumoral regions and the rest of the brain. Interestingly, we observed that functional connectivity increases after tumor resection in peritumoral regions, but not in contra-tumoral regions. Enhancement of functional connectivity emerged in the alpha frequency band and developed within 3 months after surgery. Interestingly, improvements in functional connectivity in peritumoral regions occurred regardless of the location of the brain tumor.

INTRODUCTION

Low-grade gliomas (LGGs) are slow growing brain tumors that often cause displacement and/or infiltration of healthy tissue. Unfortunately, low-grade gliomas tend to invade areas of the brain that are essential for carrying out important functions such as language processing. Brain mapping in patients with LGGs allows us to better understand neural plasticity, since we can investigate how functional reorganization occurs in these patients both before and after surgery, and how plasticity plays an important role in the recovery of brain function through compensatory mechanisms. Electrocorticographic mapping and monitoring using electrical stimulation during awake craniotomy has become the standard technique for resection of LGGs affecting language brain areas. This technique allows for accurate identification and preservation of functionally important cortical and subcortical pathways and allows for optimizing the extent of resection (EOR) while preserving quality of life (Gil-Robles and Duffau, 2010; Duffau et al., 2003a, 2003b; Satoer *et al*., 2016). In particular, Duffau *et al.*, 2003b analyzed data from a series of 103 patients who underwent surgery for LGGs located in language brain areas with the aid of intraoperative electrical mapping. Their study showed that this technique led to a very high rate of immediate postoperative worsening (80%) due to perilesional edema (Gil-Robles and Duffau, 2010). Importantly, cognitive and language difficulties were transient (1 – 2 weeks) such that 94% of patients recovered their preoperative status within 3 – 6 months and then returned to a normal socio-professional life. Results from these studies suggest that brain plasticity within 3 – 6 months after LGG resection may underlie postoperative functional recovery.

Functional neuroimaging techniques have been widely used to investigate the reorganization of language areas after LGG resection. Previous functional magnetic resonance imaging (fMRI) and positron emission tomography (PET) studies in patients with LGGs in language areas has

suggested that recovery from postoperative difficulties is associated with functional compensation by healthy peritumoral and contra-tumoral regions (Graveline *et al.*, 1998; Duffau *et al.*, 2003a, 2003b; Krainik *et al.*, 2004; Sarubbo *et al.*, 2012; Deng *et al.*, 2015; Kośla *et al.*, 2015; Kristo *et al.*, 2015). For example, language recovery following left dominant temporal resection could be related to the progressive involvement of peritumoral areas—such as the posterior part of the superior temporal gyrus (Weiller *et al.*, 1995)—and contra-tumoral regions (Karbe *et al.*, 1997; Heiss *et al.*, 1999). Most studies seem to agree that neural plasticity in peritumoral and contra-tumoral regions facilitates postoperative functional recovery after LGG resection, but they attribute varying degrees of significance to each of these regions (Heiss *et al.*, 1999; Duffau *et al.*, 2003a; Noppeney *et al.*, 2005; Gil-Robles *et al.*, 2008). The location and the size of the activated region may depend on many factors, including the amount of effort expended by the patient or the extent to which study paradigms reliably activate the brain area of interest.

Both functional MRI and PET techniques indirectly measure neuronal activity by detecting changes in blood flow (hemodynamic response) and metabolism. Electroencephalography (EEG) and magnetoencephalography (MEG) techniques directly record neural activity from the cerebral cortex. One important advantage of using EEG and MEG for patients with brain tumors is that these techniques do not have to take the influence of the tumor or effects of tumor edemas on blood supply and metabolism into account. These are factors that can lead to inaccurate functional localization in functional MRI and PET. Another advantage of EEG and MEG is the high temporal resolution which allows us detect events that occur at time scales on the order of milliseconds. Again, this differentiates EEG and MEG from both fMRI and PET, which operate at much longer time scales (seconds and minutes). Compared to EEG, MEG has excellent spatial

resolution; sources can be localized with millimeter precision. Given all these advantages, some view MEG as the best neuroimaging technique for measuring brain activity in patients with brain tumors.

MEG resting-state studies have shown plasticity in functional connectivity in diverse diseases including brain tumors, traumatic brain injury and stroke (Tarapore *et al.*, 2012; Bartolomei *et al.*, 2006; Douw *et al.*, 2008). Resting-state functional connectivity analysis makes it possible to measure changes in brain functions without depending on patient cooperation or specific activation paradigms. Overall, previous findings suggest that, in the early stages of a brain injury, functional connectivity is weaker in patients compared to controls including regions that are ipsilateral but also contralateral to the lesion (Guggisberg *et al.*, 2008; Martino *et al.*, 2011; Tarapore *et al.*, 2012, 2013). Reduced functional connectivity has been observed in the alpha frequency band. Interestingly, Tarapore and colleagues (2013) found that, within two years after brain injury, abnormally reduced post-surgical alpha functional connectivity could improve. This suggests neuroplasticity during recovery from the lesion. However, this study had several limitations. First, the time period between the brain injury and the MEG sessions varied across patients. Second, the location and extent of the injury widely varied across patients, even including lesions in both the left and the right hemispheres. Third, the study only investigated alpha-band functional connectivity. An investigation of other MEG frequency ranges such as delta (Castellanos *et al.*, 2010) and theta band (Bosma *et al.*, 2008, 2009) could provide further information regarding functional reorganization in patients with brain lesions.

In the present study, we investigate the neural mechanisms that facilitate reorganization of language networks after brain tumor resection. Functional MEG data, together with MRI structural (T1 and Diffusion Weighted Image (DWI)) and behavioral data were collected from

12 patients with LGGs in left-sided language brain areas. Data were collected before surgery (Pre session), and at 3 (Post_1 session) and 6 months (Post_2 session) after surgery. All patients underwent awake craniotomy to define cortical and subcortical functional boundaries using the no-margin technique (this technique is described in Gil-Robles and Duffau, 2010). Postoperative MRI structural data were used to identify the cortical and subcortical boundaries of the tumor resection. We measured MEG functional connectivity during eyes-closed resting-state in peritumoral and contra-tumoral (healthy regions of the right hemisphere that mirror the tumor area) regions for each patient and session. Keeping the eyes closed during the MEG resting state is clearly relevant for alpha-wave studies (Guggisberg *et al.*, 2008; Martino *et al.*, 2011; Tarapore *et al.*, 2013), and also permits us to avoid eye blink artifacts in the MEG recordings. Functional connectivity was measured in the 1 to 100 Hz frequency band using imaginary coherence (IC) (Nolte *et al*., 2004; Guggisberg *et al*., 2008; Martino *et al*., 2011; Tarapore *et al*., 2012, 2013). We hypothesized that postoperative neural plasticity occurs in peritumoral and contra-tumoral regions and develops progressively within the first 6 months after surgery (Gil-Robles and Duffau, 2010; Duffau *et al.*, 2003a, 2003b; Satoer *et al*., 2016). Thus, we expected that functional connectivity in both regions would be stronger in the Post_1 and Post_2 sessions compared to the Pre session, and in the Post_2 session compared to the Post_1 session. We also predicted that functional connectivity changes in peritumoral and contra-tumoral regions would most likely emerge in the alpha frequency band taking into account previous findings (Guggisberg *et al.*, 2008; Martino *et al.*, 2011; Tarapote *et al*., 2012, 2013).

METHODS

PARTICIPANTS

The participants were 12 patients with LGG in the left hemisphere. All patients underwent tumor surgery with awake craniotomy by the same neurosurgeons (I.P[1] and S.G.R[2]) at the Cruces University Hospital in Bilbao. Participants were referred for clinical Magnetoencephalography (MEG) scanning and MRI at the Basque Center on Cognition Brain and Language (BCBL) before surgery (Pre session) and at 3 (Post_1 session) and 6 (Post_2 session) months after surgery. Preoperative MRI data (T1 and Diffusion Weighted Image (DWI)), together with cortical and subcortical intra-operative electrical stimulation (IES) were used to identify eloquent areas during surgery. All participants were native Spanish speakers. Basic language and cognitive skills were also evaluated in each session. The BCBL and the Hospital Cruces ethical committees approved the experiment (following the principles of the Declaration of Helsinki) and all participants gave written consent to participate in the research.

Patient characteristics and clinical presentation before and after surgery are shown in Table 1. Four women and 8 men with a mean age of 39 (SE=4.19) years participated. The LGGs were located in left-sided language brain areas, including frontal (3 patients), motor (2 patient), parietal (2 patients) and temporal (5 patients) areas. All patients were right handed. All patients underwent awake craniotomy for increased lesion removal minimizing damages. A gross total (95%) resection of the tumor was achieved in 9 patients. Immediately after the surgery, all patients worked with a speech therapist to recover from language difficulties.

[1] Iñigo Pomposo; BioCruces Research Institute, Bilbao Spain.
[2] Santiago Gil-Robles; Department of Neurosurgery, Hospital Quirón, Madrid, Spain; BioCruces Research Institute,
[2] Santiago Gil-Robles; Department of Neurosurgery, Hospital Quirón, Madrid, Spain; BioCruces Research Institute, Bilbao Spain

---------- Insert Table 1 around here ----------

BEHAVIORAL DATA

The Spanish version of the Kaufman Brief Intelligence Test (KBIT) was used to measure verbal and nonverbal cognitive ability. The Cross-out task from the Woodcock-Johnson Educational Battery (Woodcock and Johnson, 1989) was used to evaluate visual scanning and attention. In this task, geometric figures were presented. Participants were asked to cross out figures that matched a target presented to the left in rows containing 21 figures each. The number of rows completed correctly (Hits) in 3 minutes and the number of errors (converted to percentages) were quantified. In addition, the Basque, English, and Spanish Test (BEST) was used to evaluate Spanish language skills (De Bruin *et al*., 2017). The BEST consists of two parts. First, expressive vocabulary was assessed through a picture-naming task on which scores can range from 0 ('lowest level') to 65 ('highest level'). Second, participants completed a 5-min semi-structured oral proficiency interview (Gollan *et al*., 2012). This interview consists of a set of questions ranging in difficulty that require the participant to use different types of grammatical constructions. The interview was conducted and assessed by a group of linguists who were native speakers of Spanish. The scoring was based on a Likert-like scale from 1 ('lowest level') to 5 ('highest level'). Not all participants completed all behavioural testing (Table 2).

MRI STRUCTURAL

Structural MRI data (T1 and Diffusion Weighted Images (DWI)) were used to identify the cortical and subcortical boundaries of the tumor resection. Furthermore, the DWI information also allowed us to identify the main tracks that connected peritumoral regions with the rest of the brain.

DATA ACQUISITION AND PREPROCESSING

All patients underwent structural MRI, in a 3.0 Tesla Siemens Magnetom Trio Tim scanner (Siemens AG, Erlangen, Germany). A high-resolution T1-weighted scan was acquired with a 3D ultrafast gradient echo (MPRAGE) pulse sequence using a 32-channel head coil and with the following acquisition parameters: FOV = 256; 160 contiguous axial slices; voxel resolution $1x1x1mm^3$; TR = 2300 ms, TE = 2.97 ms, flip angle = 9°.For each patient, the origin of the T1 weighted images (Pre, Post_1, and Post_2) was set to the anterior commissure. These images were then co-registered with each other using the mutual information algorithm implemented in Statistical Parametric Mapping (SPM8, Wellcome Department of Cognitive Neurology, London, UK). Peritumoral and contra-tumoral regions were manually defined on the individual's postoperative T1 images (Post_1 session) using MRIcro software (Rorden and Brett, 2000). Peritumoral regions contained healthy tissue within 2 cm of the tumor (Casbas-Hernandez *et al*., 2014). Contra-tumoral regions contained healthy regions of the right hemisphere that mirrored the lesioned area in the left hemisphere. The same peritumoral and contra-tumoral areas were used across sessions. Additionally, we measured the volume of the tumor before surgery (Pre tumor volume) and the volume of the tumor remaining after surgery (Post_1 tumor volume). Then, the extent of resection (EOR) was calculated for each patient as: (Pre tumor volume – Post_1 tumor volume) / Pre tumor volume.

The DWI data were acquired using a single shot echo-planar sequence with an acceleration factor of two and the following parameters: TR: 9300 ms, TE: 99 ms, FOV: 230 × 230 mm, voxel size = 1.8 × 1.8 × 1.8, slice thickness: 1.8 mm, bandwidth: 1502 Hz/Px, EPI factor: 128, echo-spacing: 0.75 ms, diffusion mode MDDW, with 64 diffusion-weighted images acquired at a b-value of 1500 s/mm^2. DWI data analysis was performed using ExploreDTI

(www.exploredti.com) (Leemans *et al*., 2009). ExploreDTI was used to correct gross artifacts (i.e., signal dropouts and interleave artifacts) in DWI data. Motion artifacts and eddy current-induced geometric distortions were reduced using an affine co-registration method based on mutual information with B-spline cubic interpolation to realign the 64 non-collinear images to the b0 image (Leemans and Jones, 2009; Klein *et al*., 2010). In this correction procedure, the b-matrix was adjusted for the rotational component of subject motion to ensure correct diffusion tensor estimates. Echo-planar imaging distortions were reduced by means of B-spline cubic interpolation to register the mean b0 image to the structural space (co-registered T1 images) (Wu *et al*., 2008). Whole brain Diffusion Tensor Imaging (DTI) was performed using fiber tractography methods with a uniform seed point resolution of 2 mm^3 and a maximum deflection angle of 30 degrees. For the DTI based fiber tractography, a fractional anisotropy threshold of 0.2 was applied. Tracts passing through the peritumoral regions were plotted.

MEG FUNCTIONAL

ACQUISITION AND PREPROCESSING

Five minutes eyes-closed resting state recordings were acquired in a magnetically shielded room using the whole-scalp MEG system (Elekta-Neuromag, Helsinki, Finland). This system is equipped with a helmet-shaped array of 306 sensors, arranged in triplets of two orthogonal planar gradiometers and a magnetometer. The position of the head with respect to the sensor array was estimated at the beginning of each block using five Head Position Indicator (HPI) coils. A 3D digitizer (Fastrak Polhemus, Colchester, VA, USA) was used to define the location of each HPI coil and approximately 200 “headpoints” along the scalp, relative to the anatomical fiducials (the nasion and left and right preauricular points). Digitalization of the fiducials and

additional points were used during subsequent data analysis to spatially align the MEG sensor coordinates with T1 magnetic resonance brain images. Data were recorded at a sampling rate of 1 KHz and filtered online with a bandwidth of 0.01-330 Hz. Eye-movements were monitored with two pairs of electrodes in a bipolar montage placed on the sides of each eye—horizontal electrooculography (EOG)—and above and below the right eye (vertical EOG). Cardiac rhythm was monitored with two pairs of electrodes in a bipolar montage placed below the left clavicle and on the right side of the lumbar region. Not all participants completed all MEG sessions. Eleven participants took part in the first MEG session, 12 in the second MEG session, and 10 in the third MEG session.

To remove external magnetic noise from the MEG recordings, data were preprocessed offline using the Signal-Space-Separation method (Taulu *et al*., 2005) implemented in Maxfilter 2.1 (Elekta-Neuromag). MEG data were also corrected for head movements, and bad channels were substituted using interpolation algorithms implemented in the software. Subsequent analyses were performed using Matlab R2010 (Mathworks, Natick, MA, USA). Heartbeat and EOG artifacts were automatically detected using Independent Component Analysis (ICA) and linearly subtracted from a concatenated file. The ICA decomposition was performed using the FastICA algorithm (Hyvärinen and Oja, 2000).

MEG SOURCE ESTIMATION

Using the MNE suite (Martinos Center for Biomedical Imaging, Massachusetts, USA), the digitized points from Polhemus were co-registered to the skin surface. The source space was defined as a regular 3D grid with 5 mm resolution and the lead fields (forward computation) were performed using a realistic three-shell model. Individual T1-weighted MRI images were

segmented into scalp, skull, and brain components using the segmentation algorithms implemented in Freesurfer (Martinos Center for Biomedical Imaging). The noise covariance matrix was estimated from empty room MEG data acquired right before bringing the patient into the MEG room. The noise covariance matrix was used to whiten the forward matrix and the data (Lütkenhöner, 1998; Lin *et al*., 2006). Finally, whole brain source activity was estimated using the L2 minimum-norm estimate (MNE) (Hämäläinen and Ilmoniemi, 1994).

FUNCTIONAL CONNECTIVITY ANALYSIS

Functional connectivity between source activity in the peritumoral and contra-tumoral regions (x(t)) and the rest of the source space (y(t)) was estimated using imaginary coherence (IC) (Nolte *et al*., 2004). Source reconstructed time-series were transformed into frequency power spectra by applying a Fast Fourier Transformation (FFT) to 2 s MEG data epochs with 1 s overlap. IC between a given source pair was calculated in the 1 – 100 Hz frequency band with 1 Hz frequency resolution according to the formula:

$$IC_{XY}(f) = \left| \mathrm{Im} \frac{\sum_{k=1}^{K} X_k(f) Y_k^*(f)}{\sqrt{\sum_{k=1}^{K} |X_k(f)|^2 \sum_{k=1}^{K} |Y_k(f)|^2}} \right|_f ,$$

where $f \in [1\,;100]$ and X_k and Y_k are the FFT of the kth segment. The absolute value of IC was used to estimate the magnitude of connectivity at each voxel. Following this procedure, IC values were obtained for each patient, MEG session, frequency and source pair. The mean IC ($\overline{IC}$) at each source was estimated by averaging all its Fisher's Z-transformed connections (Nolte *et al*. 2004):

$$\overline{IC}(f) = tanh\left(\frac{1}{C}\sum_C tanh^{-1} IC(f)\right)$$

Finally, we calculated average $\overline{IC}$ values across all the sources in peritumoral and contra-tumoral regions.

STATISTICAL ANALYSIS

We conducted an analysis of variance (ANOVA) on the behavioral and brain functional measures using SPSS software version 19.0 (SPSS, UK).

For the behavioral data, ANOVAs with session (Pre, Post_1, Post_2) as within-patient factor were conducted separately on the measures obtained in the KBIT (verbal and non-verbal IQ), Cross-out (hits and errors) and BEST (vocabulary and interview scores) for all patients.

Statistical analysis of the functional data was computed at the group and patient levels:

For the group-level statistical analysis, we used ANOVAs to identify frequency bins ($f \in [1\,;100]$) showing significant connectivity changes in peritumoral and contra-tumoral regions across time. For each frequency bin, ANOVAs with session (Pre, Post_1, Post_2) as the within-patient factor were conducted separately on the mean $\overline{IC}$ in peritumoral and contra-tumoral regions. The resulting probabilities were corrected for multiple testing by using the false discovery rate (FDR). Additionally, we calculated the average of the $\overline{IC}$ values in the frequency band of interest for each region and session. For each region, Bonferroni post-hoc tests were used to compare the averaged $\overline{IC}$ values between different sessions.

For the patient-level statistical analysis, the average of functional connectivity maps within the frequency of interest was calculated for each patient. Then, $\overline{IC}$ values in peritumoral and contra-tumoral were compared between the Post (separately for the Post_1 and Post_2) and the Pre sessions using two-tailed t-tests for one sample. We tested the null hypothesis that the

connectivity $\overline{IC}$ between a given source in the peritumoral and contra-tumoral and the rest of the source space in the Post sessions was equal to the mean of the $\overline{IC}$ values between all sources in the peritumoral and contra-tumoral and the rest of the source space in the Pre session.

Finally, we computed Pearson's correlations between the postoperative changes (Post_1 – Pre, Post_2 – Pre, Post_2 – Post_1) in the behavioral and the $\overline{IC}$ values in peritumoral and contra-tumoral regions.

RESULTS

BEHAVIORAL

Table 2 presents the behavioral assessments for all participants and sessions. All patients had immediate postoperative language or/and cognitive difficulties (1-2 weeks). Importantly, recovery occurred within 3 months in all patients. No significant effect of session emerged on the verbal ($F(2,16)=0.68$, $p=0.52$, $\eta_p^2=0.07$) and the non-verbal ($F(2,16)=3.58$, $p>0.05$, $\eta_p^2=0.18$) IQ measures of the KBIT, or on the cross-out scores (Hits: $F(2,16)=0.73$, $p=0.05$, $\eta_p^2=0.03$; Errors: $F(2,16)=0.65$, $p=0.53$, $\eta_p^2=0.03$). No significant effect of session emerged for the vocabulary ($F(2,16)=1.06$, $p=0.37$, $\eta_p^2=0.09$) and the interview scores.

---------- Insert Table 2 around here ----------

FUNCTIONAL CONNECTIVITY

We used Imaginary Coherence (IC) to evaluate the functional connectivity of peritumoral and contra-tumoral regions to the rest of the brain in the 1 – 100 Hz frequency band and for each session (Pre, Post_1 and Post_2). Results from the group-level statistical analysis (ANOVA) of

$\overline{IC}$ values showed a main effect of session ($F(2,16)=7.34$, $p<0.01$, $\eta_p^2=0.65$) only in peritumoral regions and within the alpha (9–11 Hz) frequency band (Figure 1a). For the following analyses, the average of the $\overline{IC}$ values in peritumoral regions was calculated in the alpha frequency band. Post-hoc tests (Bonferroni) showed that alpha $\overline{IC}$ values were significantly higher in the Post_1 ($p_{bonferroni}=0.02$) and the Post_2 ($p_{bonf.}=0.04$) compared to the Pre session, but not in the Post_1 compared to the Post_2 session ($p_{bonf.}=0.5$).

---------- Insert Figure 1 around here ----------

Additionally, we computed correlations between postoperative changes (Post_1 – Pre, Post_2 – Pre, Post_2 – Post_1) in the behavioral and the alpha $\overline{IC}$ values in peritumoral and contra-tumoral regions (Supplementary Table 1). No significant correlations were observed between the behavioral and the functional data (all |Pearson´s correlation (r) values|<0.69, uncorrected ps>0.06).

Finally, we analyzed the postoperative functional connectivity changes within each patient. Functional connectivity was evaluated in peritumoral and contra-tumoral regions in the alpha frequency band (9–11 Hz). Here, we describe postoperative alpha functional connectivity changes in four representative patients with LGGs in left frontal (Figure 2), motor (Figure 3), parietal (Figure 4) and temporal (Figure 5) regions.

Patient with a LGG in left frontal region

Patient 2 was a 56-year-old right-handed man with a LGG (Volume=25.74 cm^3) in the left frontal lobe that included Broca's area (BA44 and BA45). The patient underwent awake craniotomy and a gross total (95%) resection of the tumor volume was achieved (Table 1). The

resection limits extended to the superior longitudinal fasciculus (SLF) (Figure 2a). Language (Vocabulary=65, Interview=5) and cognitive performance (verbal IQ >34, non-verbal IQ >45, cross-out Hits>86, cross-out Errors=0) were normal in all sessions. We observed that the alpha $\overline{IC}$ values in peritumoral areas were significantly higher in the Post_1 (3 months after surgery) session and the Post_2 (6 months after surgery) session compared to the Pre (before) session. This functional connectivity enhancement was located in middle frontal areas (BA46) and in the medial surface of the temporal lobe (BA48) (Figure 2b). No significant differences between sessions were observed for the alpha $\overline{IC}$ values in contra-tumoral areas.

---------- Insert Figure 2 around here ----------

Patient with a LGG in left motor regions

Patient 4 was a 54-year-old right-handed man with a tumor (Vol=14.61 cm^3) in the left supplementary motor regions (BA6) (Table 1). The patient underwent awake craniotomy and a gross total (99%) resection of the tumor was achieved (Table 1). The resection limits extended to the corticospinal tracts (CST) (Figure 3a). Language (Vocabulary>63, Interview=5) and cognitive performance (verbal IQ >47, non-verbal IQ >12, cross-out Hits>23, cross-out Errors<10) were normal in all sessions. We observed that alpha $\overline{IC}$ values in peritumoral areas were significantly higher in the Post_1 session and the Post_2 session compared to the Pre session. The functional connectivity enhancement was located in BA8 and remaining regions in BA6 (Figure 3b). No significant differences between sessions were observed for the alpha $\overline{IC}$ values in contra-tumoral areas.

---------- Insert Figure 3 around here ----------

Patient with a LGG in parietal regions

Patient 6 was a 58-year-old right-handed man with a LGG (Vol=12.21cm^3) in the left intraparietal sulcus (IPS) (Table 1). The patient underwent awake craniotomy and a partial (82%) resection of the tumor was achieved (Table1). The resection limits extended to the intraparietal U-shape fibers connecting the superior and inferior parietal gyri (Zhang *et al*., 2014; Catani *et al*., 2017) (Figure 4a). Language (Vocabulary>63, Interview=5) and cognitive performance (verbal IQ >97, non-verbal IQ >68, cross-out Hits>50, cross-out Errors<3) were normal in all sessions. We observed that alpha $\overline{IC}$ values in peritumoral areas were significantly higher in the Post_1 session and the Post_2 session compared to the Pre session (Figure 4b). The functional connectivity enhancement was located in the inferior parietal lobule (BA40) and the superior parietal lobule (BA7). No significant differences between sessions were observed for the alpha $\overline{IC}$ values in contra-tumoral areas.

---------- Insert Figure 4 around here ----------

Patient with a LGG in left temporal regions

Patient 8 was a 26-year-old right-handed man with a LGG (Vol=31.09 cm^3) in the left temporal pole (Table 1), including BA38 and the anterior regions in the temporal lobe (BA20 and BA21). The patient underwent awake craniotomy and a partial (64%) resection of the tumor was achieved (Table 1). The resection limits extended to the inferior longitudinal fasciculus (ILF) inferiorly and the inferior fronto-occipital fasciculus (IFOF) superiorly (Figure 5a). Language (Vocabulary=65, Interview=5) and cognitive performance (verbal IQ >47, non-verbal IQ >68, cross-out Hits>86, cross-out Errors=0) were normal in all sessions. We observed that alpha $\overline{IC}$ values in peritumoral areas were significantly higher in the Post_1 session and the Post_2 session compared to the Pre session. The functional connectivity enhancement was located in middle and

posterior parts of the BA20 and BA21 regions (Figure 5b). No significant differences between sessions were observed for the alpha $\overline{IC}$ values in contra-tumoral areas.

---------- Insert Figure 5 around here ----------

DISCUSSION

In the present study we showed that language brain areas can be removed without incurring a permanent deficit thanks to mechanisms for brain plasticity (Duffau, 2009; Duffau *et al.*, 2003a). We used resection with no-margin together with the repetition of both cortical and subcortical stimulation to preserve eloquent cortex as well as white matter tracts (Gil-Robles and Duffau, 2010). As expected, immediate (1-2 weeks) post-surgery language and cognitive difficulties were observed in all patients due to perilesional edema (Gil-Robles and Duffau, 2010). Importantly, all our patients recovered from postoperative deficits within 3 months (Satoer *et al.*, 2016). The cognitive (verbal and non-verbal IQ) and language (Vocabulary and Interview) measures obtained before and after surgery were not significantly different.

Previous studies in patients with LGGs in eloquent brain areas suggested that postoperative functional compensation occurred mainly in peritumoral and in contra-tumoral regions (Seitz *et al.*, 1995; Heiss *et al.*, 1999; Thiel *et al.*, 2001; Duffau *et al.*, 2003a; Krainik *et al.*, 2004; Noppeney *et al.*, 2005; Gil-Robles *et al.*, 2008; Sarubbo *et al.*, 2012; Kośla *et al.*, 2015). Here, we found that postoperative functional compensations emerged only in peritumoral regions (Figure 1b). Functional alpha connectivity in peritumoral areas was significantly higher in the Post_1 and Post_2 sessions than the Pre session. However, alpha functional connectivity values in contra-tumoral areas did not differ between sessions (Figure 1b). This result does not mean that functional compensation in contra-tumoral areas does not occur in patients with LGG.

Functional compensation in contra-tumoral regions may develop before surgery and may be crucial to maintaining functions intact in spite of the presence of an LGG in language brain areas (Holodny *et al*., 2002).

We showed that functional reorganization of peritumoral areas developed within 3 months after surgery. Postoperative alpha functional connectivity in peritumoral regions at 3 and 6 months did not differ. This delay in functional reorganization suggests that neosynaptogenesis, associated with sprouting of axons and dendrites in peritumoral regions, may represent the main mechanism for plasticity, as described in vitro and in animals (Bach-y-Rita, 1990; Jacobs and Donoghue, 1991; Sanes *et al*., 1992; Duffau et al., 2003a, 2003b). Regeneration and the reorganization of neural circuits within peritumoral regions may increase interactions between these regions and the rest of the brain, and lead to higher functional connectivity values. Functional connectivity differences may emerge in the alpha frequency band because alpha neural oscillations mediate both corticocortical and thalamocortical connections (Bollimunta *et al*., 2011; Hindriks *et al*., 2014), and are the strongest brain signals during the resting state. Further research is needed to understand the links between postoperative functional and structural connectivity changes in patients with LGG.

No significant correlations were observed between postoperative changes in behavioral and functional connectivity values in peritumoral and contra-tumoral regions. This lack of correlation could be due to the fact that there was not enough variability in behavioral responses, yielding only a few data points; many patients were asymptosmatic before surgery and seemed to have fully recovered after 3 months. Finally, it might be the case that the brain changes preceded behavioral changes; the former were detected, but the latter had not yet occurred.

Postoperative functional reorganization in peritumoral regions may be a general mechanism of brain plasticity. We observed that functional reorganization in peritumoral regions occurred in LGGs located in frontal (Broca's area) (Figure 2b), motor (supplementary motor) (Figure 3b), parietal (intraparietal sulcus) (Figure 4b) and temporal (temporal pole) (Figure 5b) regions. The preservation of white matter tracts (long-distance connectivity and U-fiber white tracts) may be critical for plasticity in these regions (Gil-Robles and Duffau, 2010). Previous studies have shown that in cases of white matter injury, the risk of inducing permanent deficits without functional recovery is very high (Duffau, 2009).

Broca's area resection

Historically, Broca's area (BA44 and BA45) has been assumed to play a key role in speech production (Broca, 1861; Geschwind, 1967). In line with recent studies, we showed that Broca's area may not be systematically essential for language (Etard *et al*., 2000; Thiel *et al*., 2001; Duffau *et al*., 2003a). Thiel and colleagues (2001) showed that in cases where the LGG invaded Broca's area, functional replacement occurred in peritumoral areas of left frontolateral regions—such as BA 46 and BA 47. Similarly, we found a functional recruitment of Broca's area in middle frontal areas (BA46) and the medial surface of the temporal lobe (BA48) (Figure 2b). Preservation of the arcuate fasciculus (AF) and the superior longitudinal fasciculus (SLF) (Figure 2a) may be crucial for plasticity in Broca's area. Previous studies in patients with LGG showed that lesions in long arcuate fibers cause dysgraphia, and damage to the horizontal fibers of the SLF results in dysarthria (Maldonado *et al*., 2011).

Resection of supplementary motor regions

Supplementary motor areas (SMA) (BA6) are largely involved in speech communication and language processing (Hertrich *et al*., 2016). We confirmed the results of previous studies

showing that compensation of motor function could be explained by recruitment of peritumoral regions (BA8) (Duffau, 2001; Duffau and Capelle, 2001; Duffau *et al*., 2003a) (Figure 3b). Preservation of the corticospinal tract (CST) (Figure 3a) may be crucial for brain plasticity in SMA. Previous studies in patients have demonstrated that structural integrity of CST motor fibers revealed by DTI correlated with motor impairment (in patients with LGG, Gao *et al*., 2017; in patients with subcortical stroke, Lindenberg *et al*., 2010).

Resection of the intraparietal sulcus

The intraparietal sulcus (IPS) has been widely associated with sensorimotor functions (Andersen and Buneo, 2002) and attentional mechanisms in multiple sensory domains (Colby *et al*. 1996; Anderson *et al*. 2010). Previous studies showed that compensation of functions performed in the IPS may be explained by recruitment of brain areas within the parietal lobe (Duffau *et al*., 2002), in this case, the inferior parietal lobule (BA40) and superior parietal lobule (BA7) (Figure 4b). The preservation of intraparietal U-shape fibers (Zhang *et al*., 2014; Catani *et al*., 2017) (Figure 4a) may be crucial for post-surgical recovery in connectivity between the superior and inferior parietal gyrus and improved brain plasticity within the parietal lobe.

Resection of the left temporal pole

The left temporal pole (BA38) has been largely involved in speech semantic processing (Noppeney and Price, 2002) and speech comprehension (Giraud *et al*., 2004). Language compensation following left dominant temporal resection could be explained by the recruitment of areas adjacent to the surgical cavity (Karbe *et al*., 1997; Heiss *et al*., 1999). Along these lines, we observed that compensation of functions in the left temporal pole could be explained by recruitment of different brain regions in the temporal lobe (BA20 and BA21) (Figure 5b).

Preservation of the inferior longitudinal fasciculus (ILF) and inferior fronto-occipital fasciculus (IFOF) may be crucial for post-surgical recovery of neural plasticity in temporal regions (Figure 5a). Studies using subcortical electrical stimulation during awake surgery demonstrated that paraphasia was generated by stimulating the IFOF, whereas alexia was elicited by stimulating the ILF (Almairac *et al*., 2014; Chan-Seng *et al*., 2014).

CONCLUSIONS

This study indicates that a general mechanism for brain plasticity triggers postoperative language reorganization in peritumoral regions, but not in contra-tumoral regions. We found that functional connectivity changes occurred in peritumoral regions (and not in contra-tumoral regions) in the alpha frequency band within 3 months after surgery, regardless of the location of the brain tumor. Furthermore, we suggest that preservation of subcortical connectivity may be crucial for efficient brain plasticity (Gil-Robles and Duffau, 2010). In sum, these results are in line with concepts in brain connectomics and neuroplasticity but break with the traditional localizationist view of cerebral processing. Future large-scale studies are needed to further investigate these findings and to examine the utility of MEG as a predictive biomarker for neural plasticity in patients with LGG.

ACKNOWLEDGEMENTS

The following experiment was performed in accordance to the Ethics of the World Medical Association (Declaration of Helsinki). This research was supported in part by the Basque Government through the BERC 2018-2021 program; the Spanish State Research Agency through BCBL Severo Ochoa excellence accreditation SEV-2015-0490; the ERC-2011-ADG-295362 from the European Research Council and PSI2015-67353-R from the MINECO MC.

The authors would like to acknowledge the following individuals: First and foremost we would like to acknowledge the patients and families who participated in this study. We would also like to thank the medical and support staff of the Department of Neurosurgery at the Hospital Universitario Cruces. Finally, we would like to thank the whole BCBL research center for the constant support for our research.

REFERENCES

Almairac F, Herbet G, Moritz-Gasser S, Duffau H (2014) Parietal network underlying movement control: disturbances during subcortical electrostimulation. Neurosurgical Review 37(3):513-7.

Andersen RA, Buneo CA (2012) Intentional maps in posterior parietal cortex. Annual Review of Neuroscience 25(1):189-220.

Anderson JS, Ferguson MA, Lopez-Larson M, Yurgelun-Todd D (2010) Topographic maps of multisensory attention. Proceedings of the National Academy of Sciences 107(46):20110-4.

Bach-y-Rita P (1990) Brain plasticity as a basis for recovery of function in humans. Neuropsychologia 28(6):547-54.

Bartolomei F, Bosma I, Klein M, Baayen JC, Reijneveld JC, Postma TJ, *et al*. (2006) Disturbed functional connectivity in brain tumour patients: evaluation by graph analysis of synchronization matrices. Clinical Neurophysiology 117(9): 2039-2049.

Bollimunta A, Mo J, Schroeder CE, Ding M (2011) Neuronal mechanisms and attentional modulation of corticothalamic alpha oscillations. Journal of Neuroscience 31(13):4935-43.

Bosma I, Douw L, Bartolomei F, Heimans JJ, van Dijk BW, Postma TJ, *et al*. (2008) Synchronized brain activity and neurocognitive function in patients with low-grade glioma: a magnetoencephalography study. Neuro-Oncology 10(5): 734-744.

Bosma I, Reijneveld JC, Klein M, Douw L, Van Dijk BW, Heimans JJ, Stam CJ (2009) Disturbed functional brain networks and neurocognitive function in low-grade glioma patients: a graph theoretical analysis of resting-state MEG. Nonlinear Biomedical Physics 3(1): 9.

Broca P (1861) Remarks on the seat of the faculty of articulated language, following an observation of aphemia (loss of speech). Bulletin de la Société Anatomique 6:330-57.

Casbas-Hernandez P, Sun X, Roman-Perez E, D'arcy M, Sandhu R, Hishida A, *et al*. (2014) Tumor intrinsic subtype is reflected in cancer-adjacent tissue. Cancer Epidemiology and Prevention Biomarkers 24(2): 406-414.

Castellanos NP, Paul N, Ordonez VE, Demuynck O, Bajo R, Campo P, *et al*. (2010) Reorganization of functional connectivity as a correlate of cognitive recovery in acquired brain injury. Brain 133(8): 2365-2381.

Catani M, Robertsson N, Beyh A, Huynh V, de Santiago Requejo F, Howells H, *et al*. (2017) Short parietal lobe connections of the human and monkey brain. Cortex 97:339-57.

Chan-Seng E, Moritz-Gasser S, Duffau H (2014) Awake mapping for low-grade gliomas involving the left sagittal stratum: anatomofunctional and surgical considerations. Journal of Neurosurgery 120(5):1069-77.

Colby CL, Duhamel JR, Goldberg ME (1996) Visual, presaccadic, and cognitive activation of single neurons in monkey lateral intraparietal area. Journal of Neurophysiology 76(5):2841-52.

De Bruin A, Carreiras M, Duñabeitia JA (2017) The BEST dataset of language proficiency. Frontiers in Psychology 8:522.

Deng X, Zhang Y, Xu L, Wang B, Wang S, Wu J, *et al* (2008) Comparison of language cortex reorganization patterns between cerebral arteriovenous malformations and gliomas: a functional MRI study. Journal of Neurosurgery 122(5): 996-1003.

Douw L, Baayen H, Bosma I, Klein M, Vandertop P, Heimans J, *et al* (2008) Treatment-related changes in functional connectivity in brain tumor patients: a magnetoencephalography study. Experimental Neurology 212(2): 285-290.

Duffau H (2001) Acute functional reorganisation of the human motor cortex during resection of central lesions: a study using intraoperative brain mapping. Journal of Neurology, Neurosurgery & Psychiatry 70(4):506-13.

Duffau H (2009) Does post-lesional subcortical plasticity exist in the human brain? Neuroscience Research 65(2):131-5.

Duffau H, Capelle L (2001) Récupération fonctionnelle apres résection de gliomes infiltrant l'aire somato-sensorielle primaire (SI): étude par stimulations électriques per-opératoires. Neuro-Chirurgie 47:534-41.

Duffau H, Denvil D, Lopes M, Gasparini F, Cohen L, Capelle L, *et al*. (2002) Intraoperative mapping of the cortical areas involved in multiplication and subtraction: an electrostimulation study in a patient with a left parietal glioma. Journal of Neurology, Neurosurgery & Psychiatry 73(6):733-8.

Duffau H, Capelle L, Denvil D, Sichez N, Gatignol P, Lopes M, *et al*. (2003a) Functional recovery after surgical resection of low grade gliomas in eloquent brain: hypothesis of brain compensation. Journal of Neurology, Neurosurgery & Psychiatry 74(7):901-7.

Duffau, H., Capelle, L., Denvil, D., Sichez, N., Gatignol, P., Taillandier, L, *et al.* (2003b). Usefulness of intraoperative electrical subcortical mapping during surgery for low-grade gliomas located within eloquent brain regions: functional results in a consecutive series of 103 patients. Journal of Neurosurgery 98(4):764-778.

Etard O, Mellet E, Papathanassiou D, Benali K, Houdé O, Mazoyer B, *et al*. (2000) Picture naming without Broca's and Wernicke's area. Neuroreport 11(3):617-22.

Gao B, Shen X, Shiroishi MS, Pang M, Li Z, Yu B, *et al*. (2017) A pilot study of preoperative motor dysfunction from gliomas in the region of corticospinal tract: Evaluation with diffusion tensor imaging. PloS One 12(8):e0182795.

Geschwind N (1967) The varieties of naming errors. Cortex 3(1):97-112.

Gil-Robles S, Duffau H (2010) Surgical management of World Health Organization Grade II gliomas in eloquent areas: the necessity of preserving a margin around functional structures. Neurosurgical Focus 28(2):E8.

Gil-Robles S, Gatignol P, Lehéricy S, Duffau H (2008) Long-term brain plasticity allowing a multistage surgical approach to World Health Organization Grade II gliomas in eloquent areas: report of 2 cases. Journal of Neurosurgery 109(4): 615-624.

Giraud AL, Kell C, Thierfelder C, Sterzer P, Russ MO, Preibisch C, *et al*. (2004) Contributions of sensory input, auditory search and verbal comprehension to cortical activity during speech processing. Cerebral Cortex 14(3):247-55.

Gollan TH, Weissberger GH, Runnqvist E, Montoya RI, Cera CM (2012) Self-ratings of spoken language dominance: A Multilingual Naming Test (MINT) and preliminary norms for young and aging Spanish–English bilinguals. Bilingualism: Language and Cognition 15(3):594-615.

Graveline CJ, Mikulis DJ, Crawley AP, and Hwang PA (1998) Regionalized sensorimotor plasticity after hemispherectomy fMRI evaluation. Pediatric Neurology 19(5): 337-342.

Guggisberg AG, Honma SM, Findlay AM, Dalal SS, Kirsch HE, Berger MS, *et al*. (2008) Mapping functional connectivity in patients with brain lesions. Annals of Neurology 63(2):193-203.

Hämäläinen MS, Ilmoniemi RJ (1994) Interpreting magnetic fields of the brain: minimum norm estimates. Medical & Biological Engineering & Computing 32(1):35-42.

Heiss WD, Kessler J, Thiel A, Ghaemi M, Karbe H (1999) Differential capacity of left and right hemispheric areas for compensation of poststroke aphasia. Annals of Neurology 45(4):430-8.

Hertrich I, Dietrich S, Ackermann H (2016) The role of the supplementary motor area for speech and language processing. Neuroscience & Biobehavioral Reviews 68:602-10.

Hindriks R, van Putten MJ, Deco G (2014) Intra-cortical propagation of EEG alpha oscillations. Neuroimage 103:444-53.

Holodny AI, Schulder M, Ybasco A, Liu WC (2002) Translocation of Broca's area to the contralateral hemisphere as the result of the growth of a left inferior frontal glioma. Journal of Computer Assisted Tomography 26(6):941-3.

Hyvärinen A, Oja E (2000) Independent component analysis: algorithms and applications. Neural Networks 13(4-5):411-30.

Jacobs KM, Donoghue JP (1991) Reshaping the cortical motor map by unmasking latent intracortical connections. Science 251(4996):944-7.

Karbe H, Herholz K, Kessler J, Wienhard K, Pietrzyk UE, Heiss WD (1997) Recovery of language after brain damage. Advances in Neurology 73:347-58.

Klein S, Staring M, Murphy K, Viergever MA, Pluim JP (2010) Elastix: a toolbox for intensity-based medical image registration. IEEE Transactions on Medical Imaging 29(1):196-205.

Kośla K, Bryszewsk, B, Jaskólski D, Błasiak-Kołacińska N, Stefańczyk L, and Majos, A (2015) Reorganization of language areas in patient with a frontal lobe low grade glioma–fMRI case study. Polish Journal of Radiology 80: 290.

Krainik A, Duffau H, Capelle L, Cornu P, Boch AL, Mangin JF, *et al*. (2004) Role of the healthy hemisphere in recovery after resection of the supplementary motor area. Neurology 62(8): 1323-1332.

Kristo G, Raemaekers M, Rutten GJ, de Gelder B, and Ramsey NF (2015) Inter-hemispheric language functional reorganization in low-grade glioma patients after tumour surgery. Cortex 64: 235-248.

Leemans A, Jones DK (2009) The B-matrix must be rotated when correcting for subject motion in DTI data. Magnetic Resonance in Medicine 61(6):1336-49.

Leemans A, Jeurissen B, Sijbers J, Jones DK (2009) ExploreDTI: a graphical toolbox for processing, analyzing, and visualizing diffusion MR data. InProc Intl Soc Mag Reson Med 17:3537.

Lin FH, Belliveau JW, Dale AM, Hämäläinen MS (2006) Distributed current estimates using cortical orientation constraints. Human Brain Mapping 27(1):1-3.

Lindenberg R, Renga V, Zhu LL, Betzler F, Alsop D, Schlaug G (2010) Structural integrity of corticospinal motor fibers predicts motor impairment in chronic stroke. Neurology 74(4):280-7.

Lütkenhöner B (1998) Dipole source localization by means of maximum likelihood estimation. I. Theory and simulations. Electroencephalography and Clinical Neurophysiology 106(4):314-21.

Maldonado IL, Moritz-Gasser S, Duffau H (2011) Does the left superior longitudinal fascicle subserve language semantics? A brain electrostimulation study. Brain Structure and Function 216(3):263.

Martino J, Honma SM, Findlay AM, Guggisberg AG, Owen JP, Kirsch HE, *et al*.(2011) Resting functional connectivity in patients with brain tumors in eloquent areas. Annals of Neurology 69(3):521-32.

Nolte G, Bai O, Wheaton L, Mari Z, Vorbach S, Hallett M (2004) Identifying true brain interaction from EEG data using the imaginary part of coherency. Clinical Neurophysiology 115(10):2292-307.

Noppeney U, Price CJ (2002) A PET study of stimulus-and task-induced semantic processing. Neuroimage 15(4):927-35.

Noppeney U, Price CJ, Duncan JS, Koepp MJ (2005) Reading skills after left anterior temporal lobe resection: an fMRI study. Brain 128(6):1377-85.

Rorden C, Brett M (2000) Stereotaxic display of brain lesions. Behavioural Neurology 12(4):191-200.

Sanes JN, Wang J, Donoghue JP (1992) Immediate and delayed changes of rat motor cortical output representation with new forelimb configurations. Cerebral Cortex 2(2):141-52.

Sarubbo S, Le Bars E, Moritz-Gasser S, Duffau H (2012) Complete recovery after surgical resection of left Wernicke's area in awake patient: a brain stimulation and functional MRI study. Neurosurgical Review 35(2): 287-292.

Satoer D, Visch-Brink E, Dirven C, Vincent (2016) Glioma surgery in eloquent areas: can we preserve cognition?. Acta Neurochirurgica 158(1):35-50.

Seitz RJ, Huang Y, Knorr U, Tellmann L, Herzog H, Freund HJ (1995) Large-scale plasticity of the human motor cortex. Neuroreport 6(5):742-4.

Tarapore PE, Tate MC, Findlay AM, Honma SM, Mizuiri D, Berger MS, *et al*. (2012) Preoperative multimodal motor mapping: a comparison of magnetoencephalography imaging, navigated transcranial magnetic stimulation, and direct cortical stimulation. Journal of Neurosurgery 117(2):354-62.

Tarapore PE, Findlay AM, LaHue SC, Lee H, Honma SM, Mizuiri D, *et al*. (2013) Resting state magnetoencephalography functional connectivity in traumatic brain injury. Journal of Neurosurgery 118(6):1306-16.

Taulu S, Simola J, Kajola M (2005) Applications of the signal space separation method. IEEE Transactions on Signal Processing 53(9):3359-72.

Thiel A, Herholz K, Koyuncu A, Ghaemi M, Kracht LW, Habedank B, *et al*. (2001) Plasticity of language networks in patients with brain tumors: a positron emission tomography activation study. Annals of Neurology 50(5):620-9.

Weiller C, Isensee C, Rijntjes M, Huber W, Müller S, Bier D, *et al*. (1995) Recovery from Wernicke's aphasia: a positron emission tomographic study. Annals of Neurology 37(6):723-32.

Wu M, Chang LC, Walker L, Lemaitre H, Barnett AS, Marenco S, *et al*. (2008) Comparison of EPI distortion correction methods in diffusion tensor MRI using a novel framework. In International Conference on Medical Image Computing and Computer-Assisted Intervention (pp.321-329). Springer, Berlin, Heidelberg.

Zhang T, Chen H, Guo L, Li K, Li L, Zhang S, *et al*. (2014) Characterization of U-shape streamline fibers: Methods and applications. Medical Image Analysis 18(5):795-807.

FIGURE CAPTIONS

Figure 1: Functional connectivity values. a) Spectrum of the functional connectivity (mean imaginary coherence ($\overline{IC}$)) values between 1 and 20 Hz (analyzed up to 100 Hz) in peritumoral regions before (Pre, blue) and at 3 (Post_1, green) and 6 (Post_2, red) months after the tumor resection. Frequency bins where $\overline{IC}$ values showed a main effect of session are delimited by the dotted line (9, 10 and 10 Hz). b) Mean and standard error of the mean alpha $\overline{IC}$ values in peritumoral and contra-tumoral regions within the alpha frequency (9–11 Hz) for each session.

Figure 2: DTI and alpha functional connectivity analysis in a patient with a LGG in frontal areas. a) Saggital, coronal and axial views of the DTI tracks around the tumor three months after the surgery. b) Alpha functional connectivity differences between the Post_1 (3 months after surgery) and the Pre (before surgery) sessions (left), and the Post_2 (6 months after surgery) and the Pre sessions (right) overlapped in the postoperative T1 images. Sources that present higher (hot scale) alpha functional connectivity in the Post_1 session and the Post_2 session compared to the Pre session are highlighted.

Figure 3: DTI and alpha functional connectivity analysis in a patient with a LGG in supplementary motor areas. a) Saggital, coronal and axial views of the DTI tracks around the tumor three months after the surgery. b) Alpha functional connectivity differences between the Post_1 (3 months after surgery) and the Pre (before surgery) sessions (left), and the Post_2 (6 months after surgery) and the Pre sessions (right) overlapped in the postoperative T1 images. Sources that present higher (hot scale) alpha functional connectivity in the Post_1 session and the Post_2 session compared to the Pre session are highlighted.

Figure 4: DTI and alpha functional connectivity analysis in a patient with a LGG in parietal areas. a) Saggital, coronal and axial views of the DTI tracks around the tumor three months after the surgery. b) Alpha functional connectivity differences between the Post_1 (3 months after surgery) and the Pre (before surgery) sessions (left), and the Post_2 (6 months after surgery) and the Pre sessions (right) overlapped in the postoperative T1 images. Sources that present higher (hot scale) alpha functional connectivity in the Post_1 session and the Post_2 session compared to the Pre session are highlighted.

Figure 5: DTI and alpha functional connectivity analysis in a patient with a LGG in temporal regions. a) Saggital, coronal and axial views of the DTI tracks around the tumor three months after the surgery. b) Alpha functional connectivity differences between the Post_1 (3 months after surgery) and the Pre (before surgery) sessions (left), and the Post_2 (6 months after surgery) and the Pre sessions (right) overlapped in the postoperative T1 images. Sources that present higher (hot scale) alpha functional connectivity in the Post_1 session and the Post_2 session compared to the Pre session are highlighted.

TABLES

Table 1: Patient characteristics.

Patient	Age	Sex	Educational level	Lat.	Localization	Preop. T Vol. (cm^3)	Postop. T Vol. (cm^3)	EOR (%)
1	32	M	Basic	L	Front.	25.74	1.28	95
2	56	M	Basic	L	Front.	42	2.1	95
3	14	M	Basic	L	Front.	34.21	0.34	99
4	54	M	Basic	L	Motor	14.61	0.14	99
5	32	F	Graduate	L	Motor	17.11	0.17	99
6	58	M	Basic	L	Parietal	12.21	2.19	82
7	54	F	Graduate	L	Parietal	12.76	7.1	44
8	26	M	Master's	L	Temp.	31.09	11.21	64
9	41	F	Basic	L	Temp.	34.15	1.71	95
10	33	F	Master's	L	Temp.	4.79	0.05	99
11	23	M	Graduate	L	Temp.	33.24	0.33	99
12	45	M	Basic	L	Temp.	5.11	0.05	99

Note: Abbreviations: Lat = lateralization, Preop. T Vol.= preoperative tumor volume, Postop. T Vol.= postoperative tumor volume, EOR = extent of resection, F = female, M = male, L = left, Front = Frontal, Temp.= Temporal.

Table 2: Behavioral screening.

	Pre session			Post_1 session (3 months)			Post_2 session (6 months)		
Task	N	M	SE	N	M	SE	N	M	SE
KBIT									
Verbal	12	51.17	7.44	10	52.1	10.25	9	65.22	8.55
Non-verbal	12	54.17	7.5	10	70.2	5.09	9	65.33	8.34
BEST									
Vocabulary	10	63.5	0.73	11	60.64	2.81	9	63.89	0.87
Interview	10	5	0	11	5	0	9	5	0
Cross-out									
Hits	12	66.94	5.66	11	67.88	7.11	9	72.59	6.89
Errors	12	3.05	0.87	11	6.36	2.56	9	2.22	0.78

Note: Abbreviations: N=number of patients, M=mean, SE=standard error.

Supplementary Table 1: Correlation analysis.

r, p-value		Post_1 - Pre		Post_2 - Pre	
		$\overline{IC}$ in P	$\overline{IC}$ in CT	$\overline{IC}$ in P	$\overline{IC}$ in CT
Post_1-Pre	**KBIT** *Verbal*	0.3, 0.43	-0.38, 0.31		
	KBIT *Non-verbal*	-0.25, 0.51	0.37, 0.33	-	-
	BEST *Vocabulary*	-0.05, 0.91	-0.69, 0.06	-	-
	Cross-out *Hits*	0.31, 0.38	-0.25, 0.48	-	-
	Cross-out *Errors*	-0.25, 0.48	-0.28, 0.43	-	-
Post_2- Pre	**KBIT** *Verbal*	-	-	-0.06, 0.88	-0.11, 0.79

KBIT *Non-verbal*	-	-	0.15, 0.73	0.04, 0.92
BEST *Vocabulary*	-	-	0.28, 0.59	0.35, 0.5
Cross-out *Hits*	-	-	0.43, 0.28	0.23, 0.59
Cross-out *Errors*	-	-	-0.4, 0.33	-0.39, 0.34

Note: Abbreviations: r=Pearson's correlation coefficient, $\overline{(IC)}$=Mean Imaginary Coherence, P=peritumoral, CT=contra tumoral.

Figure 1:

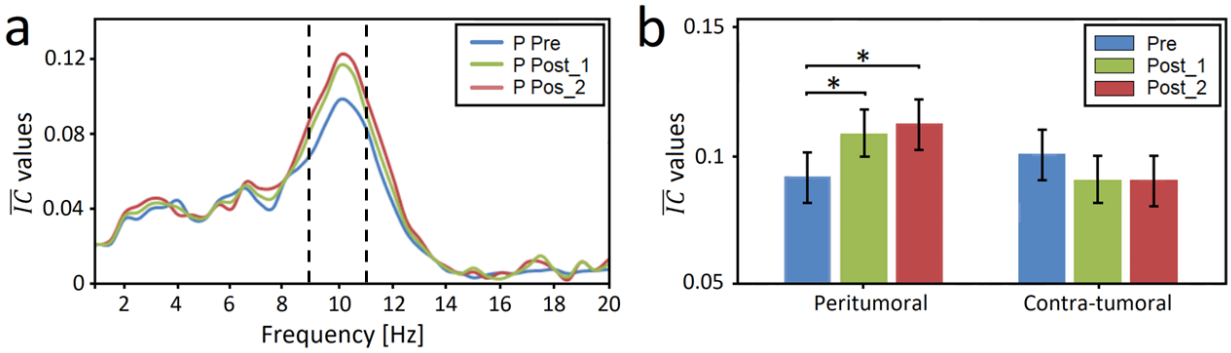

Figure 2:

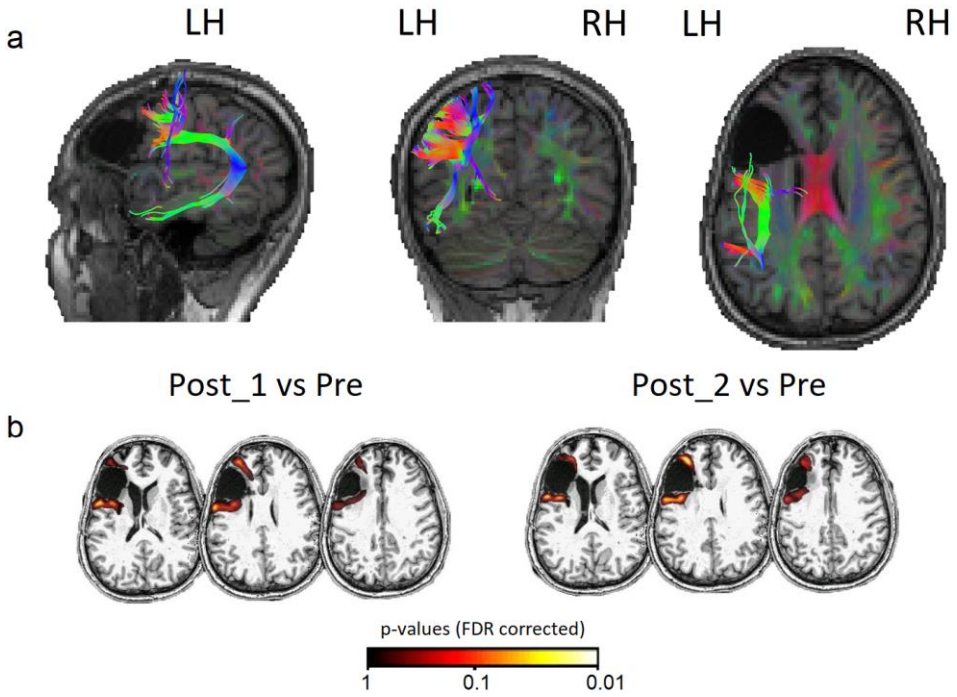

Figure 3:

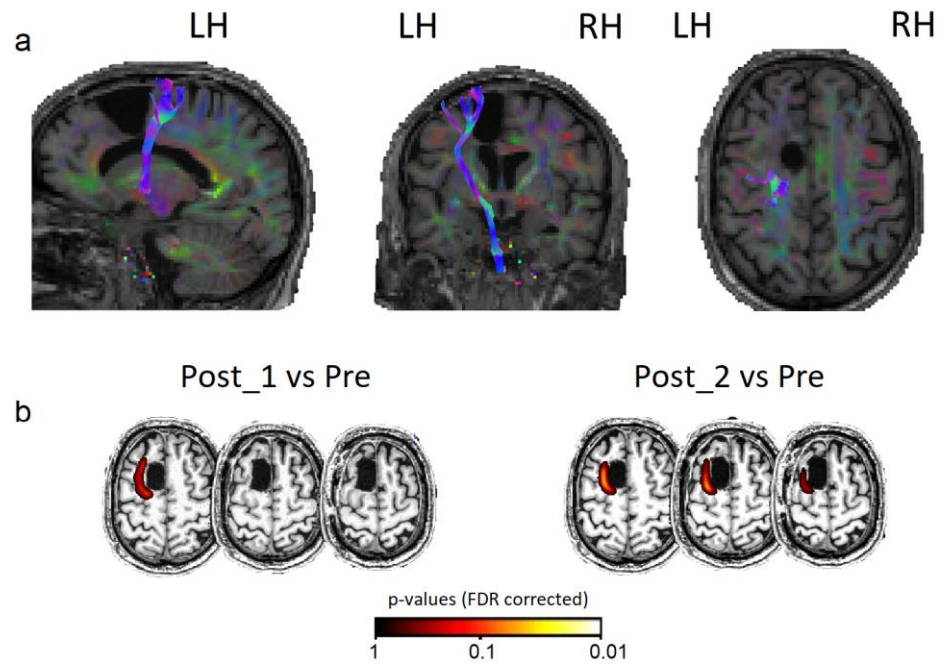

Figure 4:

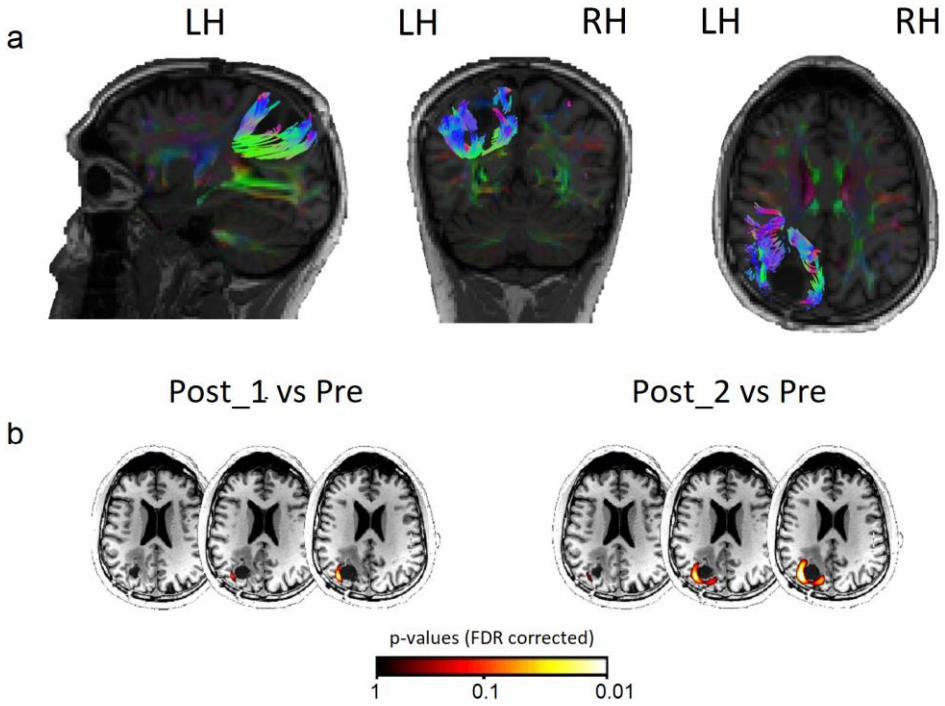

Figure 5:

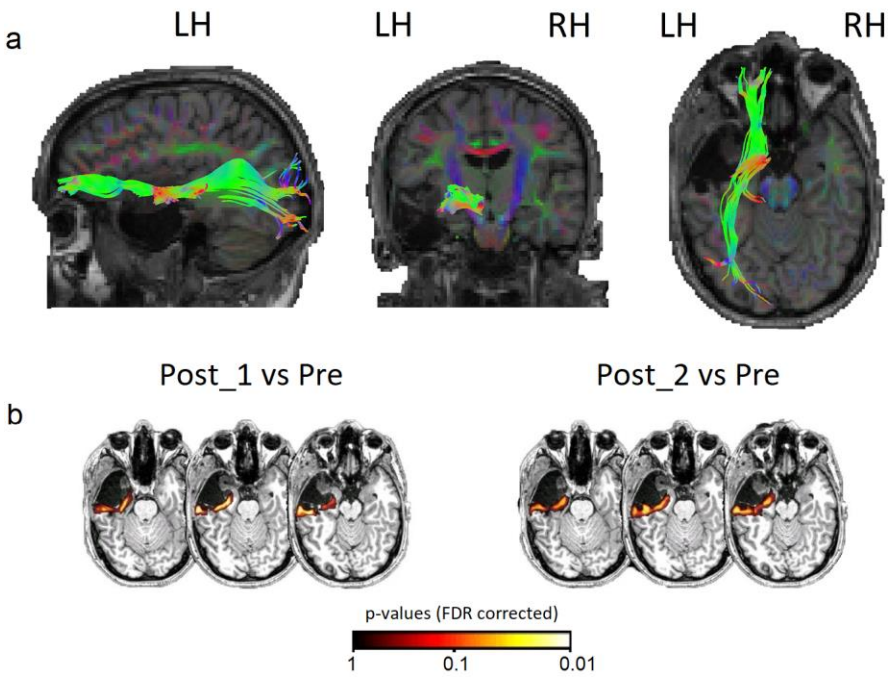
a
LH
LH
RH
LH
RH
b
Post_1 vs Pre
Post_2 vs Pre
p-values (FDR corrected)
1
0.1
0.01